Computer modelling and simulation of a novel printing head for complex tissue engineering constructs

Gokhan Ates[1,*]

[1]School of Mechanical, Aerospace and Civil Engineering, The University of Manchester, Manchester, UK

Abstract. In tissue engineering, three-dimensional functional scaffolds with tailored biological properties are needed to be able to mimic the hierarchical structure of biological tissues. Recent developments in additive biomanufacturing allow to extrude multiple materials enabling the fabrication of more sophisticated tissue constructs. These multi-material biomanufacturing systems comprise multiple printing heads through which individual materials are sequentially printed. Nevertheless, as more printing heads are added the fabrication process significantly decreases, since it requires mechanical switching among the physically separated printheads to enable printing multiple materials. In addition, this approach is not able to create biomimetic tissue constructs with property gradients. To address these limitations, this paper presents a novel static mixing extrusion printing head to enable the fabrication of multi-material, functionally graded structures using a single nozzle. Computational fluid dynamics (CFD) was used to numerically analyze the influence of Reynolds number on the flow pattern of biomaterials and mixing efficiency considering different miscible materials.

1 Introduction

Natural tissues are complex structures composed of a hierarchical multi-functional and multi-material extracellular matrix and cells. Biomanufacturing, the combined use of additive manufacturing (3D Printing), biocompatible and biodegradable materials, cells and biomolecular signals (growth factors), emerged as a suitable approach to create tissue constructs [1]. Two main strategies have been considered: scaffold-based and cell-laden. In the case of a scaffold-based approach, additive manufacturing is used to produce three-dimensional (3D) biodegradable and biocompatible porous structures (scaffolds) that provide the physical substrate for cells to attach, differentiate and proliferate. After fabrication, scaffolds are usually seeded with cells and pre-cultured in a bioreactor before implantation. In the case of a cell-laden approach, additive manufacturing is used to print bioinks (hydrogels containing cells and growth factors) allowing the fabrication of soft tissues [2]. Among the different additive manufacturing techniques currently available,

* Corresponding author: gokhan.ates@manchester.ac.uk

extrusion-based processes are the most suitable for both scaffold-based and cell-laden approaches. A wide range of printing heads (e.g. screw, pressure, or pneumatic-assisted) are being used allowing to process a wide range of materials but limited to the fabrication of single-material scaffolds or cell-laden constructs. In order to address this limitation multi-printhead systems have been developed to produce multi-material structures. Co-axial printing heads have been also developed enabling the fabrication of core-shell or hollow fibres. However, none of these systems are able to create functionally graded structures enabling the fabrication of structures based on a specific number of materials but with gradients of properties in a tailored way. In order to address this, our group is investigating the use of a Kenics mixer printing head. In order to design this printing head, it is important to understand fluid flow conditions and the mixing process in order to guarantee a good mixture of at least two materials. This paper presents preliminary results of a simplified model of the printing head considering two biocompatible and biodegradable materials. In order to create functionally graded tissue-engineered scaffolds understanding the mixing characteristic of different biomaterials is vital. CFD analysis was used to evaluated critical parameters such as mixing index, pressure drop and velocity.

2 Modelling and simulation

2.1 Static mixer printing head and simulation conditions

In this research, Kenics mixer was used as a part of printing head. It consists of a series of blades alternating clockwise and counter-clockwise twist which are arranged axially within a bifurcated pipe so that the leading edge of a blade is at right angles to the following edge of the previous blade. Blades were designed considering a twist angle of 180° and a rotation angle of 90° relative to the previous element. The aspect ratio of the Kenics blades (A*r*), which corresponds to the ratio between the length *l* and width *w* of the element, is 1.5.

The commercial CFD software ANSYS CFX 19.2 (ANSYS Inc., USA), was used to numerically analyse the flow and mixing behaviour inside printing head. Multicomponent, the steady-state, laminar, incompressible, and isothermal flows were taken into account in all simulations. The domain discretization was carried out with unstructured tetrahedral elements. Simulations were performed considering two biocompatible and biodegradable natural polymers, alginate and gelatin, commonly used in tissue engineering. Details of these two materials are shown in Table 1.

Table 1. Simulation conditions and physical properties of the two considered fluids

	Alginate (Inlet 1)	**Gelatin (Inlet 2)**
ρ: density (kg/m^3)	1255	1255
μ: viscosity (N.s.m^{-2})	0.00925	0.01
Inlet velocity range (m/s)	737×10^{-5}-1474×10^{-3}	796×10^{-5}-1593×10^{-3}
Operating temperature (^{0}C)	40	40

2.2 Governing equations

The mixing process of two miscible fluids in a modified Kenics static mixer was analysed by solving the Navier-Stokes and continuity equations in the laminar flow region. In the case of incompressible flow, the mass conservation is simplified to a volume continuity equation as follows:

$$\nabla . \mathrm{u} = 0 \tag{1}$$

where u is the fluid velocity (m/s).

The momentum conservation equation in the motionless mixer with helical segments is given by following equation:

$$\nabla . (\rho u u) = -\nabla \mathrm{p} + \nu \nabla^2 u \tag{2}$$

where ρ is the fluid density, ν is the kinematic viscosity. In the mixing process, the mass transport occurs through both diffusion and advection. Hence, the scalar transport equation of advection-diffusion type is provided as follows:

$$(u . \nabla) C = \alpha \nabla^2 C \tag{3}$$

where α is the kinematic diffusivity coefficient and C is the concentration of gelatin and alginate solutions in the static mixer.

2.3 Boundary conditions

In order to solve the governing equations of a laminar flow presented in the previous section, the following boundary conditions were imposed. Velocity boundary condition was employed for mixer inlets and the velocities are fixed for each fluids (alginate and gelatin) corresponding to the Reynolds number ranging from 10 to 2000. The Reynolds number for both entrances was defined based on the diameter of the bifurcated pipe:

$$Re = \frac{\rho V D_h}{\mu} \tag{4}$$

where ρ is density, V is the average velocity, D_h is the diameter of the pipe and μ is the dynamic viscosity of the fluid. A uniform velocity profile was assumed at each inlet. The static pressure was set to zero at the outlet and the no-slip condition was applied at the walls and on the surface of the mixing elements. A low diffusivity coefficient of 1×10^{-10} ($m^2 . s^{-1}$) [3] was assumed for gelatin so that the molecular diffusion can be neglected. In order to discretize the advection terms a high-resolution scheme of second-order approximation was employed. A converge criterion of root-mean-square (RMS) residual value of 1.0×10^{-6} was established and the number of iteration was set to 5000.

2.4 Mixing index

The distributive mixing capacity of the Kenics mixer was analysed for different Re numbers. Distributive mixing represents the spatial distribution of the components across the fluid domain and compared to dispersive mixing it is rather easier to achieve. As the distributive mixing capacity of a mixer cannot be judged depending on the visual contour plots only, it is essential to quantitatively evaluate the mixing performance. Therefore, mixing efficiency of the static mixer was analysed utilizing a statistical measurement method based on the concept of intensity of segregation. As previously reported, the mixing processes can be quantified using the mixing index (M.I) [4] at a cross-sectional plane perpendicular to flow direction, according to the following equation [1–6]:

$$M.I = \sqrt{\frac{\sigma^2}{\sigma_{max}^2}} \tag{5}$$

where σ^2 refers to actual variance, σ_{max}^2 denotes maximum possible variance at a cut-plane normal to the flow direction and σ^2 is defined as:

$$\sigma^2 = \frac{1}{n}\sum_{i=1}^{n}(c_i - \bar{c})^2 \tag{6}$$

where c_i is the mass fraction at *i*th sampling point, $\bar{c}$ is the optimal mixing mass fraction and n is the number of sampling points on the associated plane. The optimal mass fraction ($\bar{c}$) at the cut plane is equal to 0.5 for symmetrical boundary conditions. The maximum variance (σ_{max}^2) is determined from the following equation:

$$\sigma_{max}^2 = \bar{c}(1 - \bar{c}) \tag{7}$$

As the optimal maximum mass fraction $\bar{c}$ is equal to 0.5, in the case of equal flow of the fluid streams the value of σ_{max}^2 is considered to be equal to 0.25. The mixing index varies from 0 (unmixed state) to 1 (completely mixed fluid). As the mixing index decreases from 1 to 0, a lesser amount of mixing is achieved. Conversely, the higher mixing index represents higher mixing performance. However, it has been reported that the numerical results might overestimate the mixing quality due to numerical diffusion [5].

3 Results and Discussion

The influence of Reynolds number on the mass fraction distribution of both the gelatin and alginate was evaluated by plotting mass fraction contours at successive cross-sectional planes across the mixing zone. The mass fraction at the inlets was considered as reference for calculations and a step function was observed through the mixing channel width, with half of the bifurcated pipe filled with gelatin solution (red colour) and the other with alginate (blue colour) as shown in Fig.2. As the fluids flow into the mixing zone a transverse dispersion is observable at the end of each mixing element due to the stretching and folding process. The interfacial area became progressively blurred with two materials mingled together through stretching, splitting and recombining of the fluid-streams toward the complete mixing at the end of the mixer. For the lowest Reynolds number (Re=10), the thickness of the interfacial area at the cross-section before the first mixing blade is wider than those at Re=100, 500, 1000, 1500, and 2000. This can be attributed to fact that the lowest velocity results in the longest residential time of the fluids that provides the longest time for diffusion [5,7]. In order to quantitatively assess the degree of mixing, mixing index calculations were conducted across the mixing channel. Fig. 2a shows a comparison of predicted mixing indexes at the outlet of the mixer at different Re numbers. As observed, there is an inverse relationship between the Reynolds number and the mixing quality. The highest mixing index of 0.99 was achieved at Re=10, while the lowest value of 0.96 was obtained at the highest Re number. Overall, the proposed Kenics mixer for 3D Printing shows good mixing performance regardless of the Reynolds number owing to the presence of chaotic advection.

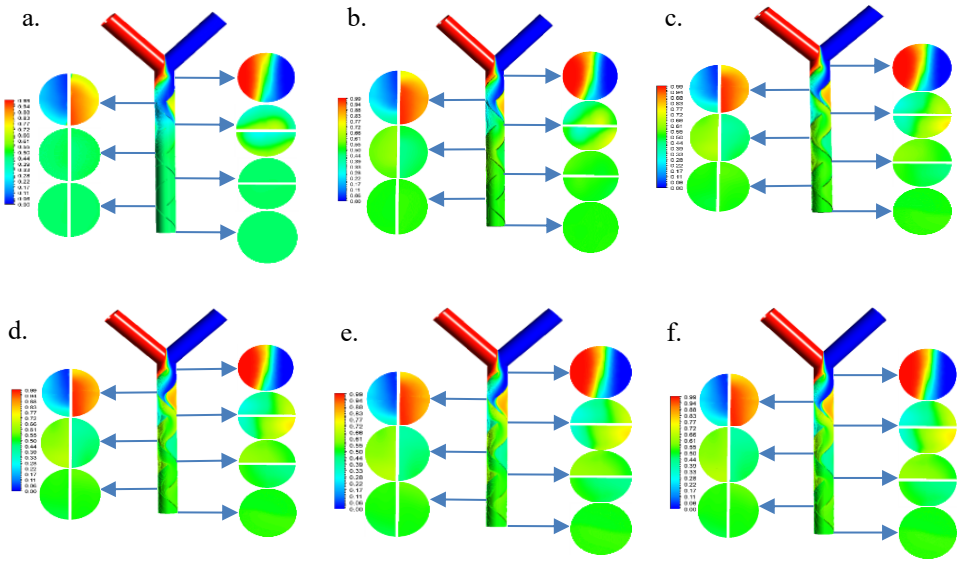

Fig. 1. Gelatin mass fraction (red colour) distributions at seven successive cross-sections and across the mixer for various Re numbers: (a) Re=10, (b) Re=100, (c) Re=500, (d) Re=1000, (e) Re=1500, and (f) Re=2000.

As the number of mixing units increases, the enhancement of the mixing index is generally smaller (Fig. 2b). After two mixing elements, the mixing index rapidly increases, and its value is higher than 0.7 over the all range of Reynolds numbers. The lowest mixing was observed at the cross-sectional plane where no mixing element is present. As the fluids proceed to the outlet the mixing index significantly increases. From Fig. 2c. it is also possible to observe that after the fourth mixing element (near to the outlet) the mixing index is almost the same for all the considered cases. This phenomenon, defined as tailpipe or downstream effects, is associated to the fact that in the case of laminar flow no further mixing takes place in this region, while in the case of turbulent flow the mixing process proceeds as the extra turbulence produced by the mixing units dies out [11].

a b. c

Fig. 2. (a) Effect of Re number on the mixing index at the outlet; the influence of the number of mixing elements on mixing performance: (b) Mixing index vs Re number, (c) Mixing index vs number of mixing units.

4 Conclusion

The flow behaviour of two miscible biomaterials in a bifurcated shape Kenics mixer was studied using a numerical method and considering different Re numbers. It was observed that splitting and recombining the fluids in a continuous manner played a significant role to achieve high levels of mixing. The highest velocity magnitude was obtained at Re=2000 with a corresponding peak pressure drop of around 100 kPa. The results show that the proposed mixer design can be used to achieve high mixing quality even at the low Reynolds numbers.

References

1. C. Mota, D. Puppi, F. Chiellini, and E. Chiellini, J. Tissue Eng. Regen. Med. **9**, 3 (2015)
2. J. Malda, J. Visser, F. P. Mechels, T. Jüngst, W. E. Hennink, W. J. A. Dhert, J. Groll, D. W. Hutmacher, Adv. Mater. **25**, 36 (2013)
3. A. Afzal and K. Y. Kim, Sensors Actuators, B Chem. **211**, 198–205 (2015)
4. M. Rafeie, M. Welleweerd, A. Hassanzadeh-Barforoushi, M. Asadnia, W. Olthuis, and M. E. Warkiani, Biomicrofluidics, **11**, 1 (2017)
5. N. Ait Mouheb, D. Malsch, A. Montillet, C. Solliec, and T. Henkel, Chem. Eng. Sci. **68**, 1 (2012)
6. I. Shah, S. W. Kim, K. Kim, Y. H. Doh, and K. H. Choi, Chem. Eng. J. **358**, 691–706 (2019)
7. J. Zhang and X. Luo, Micromachines, **9,** 5 (2018)
8. S. Sarkar, K. K. Singh, V. Shankar, and K. T. Shenoy, Chem. Eng. Process. Process Intensif. **85**, 227–240 (2014)
9. H. S. Santana, J. L. Silva, and O. P. Taranto, Chem. Eng. Sci. **132**, 159–168 (2015)
10. W. Raza, S. Hossain, and K. Y. Kim, Sensors Actuators, B Chem. **258**, 381–392 (2018)
11. E. L. Paul, V. a Atiemo-obeng, and S. M. Kresta, *Handbook of industrial mixing: Science and practice* (Hoboken: John Wiley & Sons, Incorporated, 2003)